JAERI-M
9799

OBSERVATION OF DENSITY FLUCTUATIONS BY MICROWAVE INTERFEROMETER AND SCATTERING IN THE JFT-2 TOKAMAK

November 1981

Teruaki ŚHOJI, Takumi YAMAMOTO,
Akimasa FUNAHASHI, Michiya SHIMADA,
Noboru FUJISAWA and Tomohide KAWAKAMI

日本原子力研究所
Japan Atomic Energy Research Institute

JAERI-M レポートは，日本原子力研究所が不定期に公刊している研究報告書です。
入手の問合わせは，日本原子力研究所技術情報部情報資料課（〒319—11 茨城県那珂郡東海村）あて，お申しこしください。なお，このほかに財団法人原子力弘済会資料センター（〒319-11 茨城県那珂郡東海村日本原子力研究所内）で複写による実費頒布をおこなっております。

JAERI-M reports are issued irregularly.
Inquiries about availability of the reports should be addressed to Information Section, Division of Technical Information, Japan Atomic Energy Research Institute, Tokai-mura, Naka-gun, Ibaraki-ken 319-11, Japan.

編集兼発行　日本原子力研究所
印　　刷　山田軽印刷所

JAERI-M 9799

Observation of Density Fluctuations by Microwave Interferometer and Scattering in the JFT-2 Tokamak

Teruaki SHOJI, Takumi YAMAMOTO, Akimasa FUNAHASHI,
Michiya SHIMADA+, Noboru FUJISAWA+ and Tomohide KAWAKAMI

Division of Thermonuclear Fusion Research,
Tokai Research Establishment, JAERI

(Received October 21, 1981)

Density fluctuations of micro-instability that concern with anomalous transports in Tokamak have been measured by two methods; interferometer and scattering system of 4 mm microwave. Its maximum amplitude measured by interferometer, $\tilde{n}_{emax}/n_e$, is of the order of 10^{-2} and the amplitude with wave number $k_\perp \simeq 28.6$ cm^{-1} measured by scattering method is of the order of 10^{-3}. The diffusion coefficient estimated by using DTEM theory from the desity fluctuation is of the order of the experimental value. The density dependence of diffusion coefficient, $D \propto 1/n_e$, which is derived from the density dependence of the fluctuation amplitude and the growth rate of DTEM, is consistent with the empirical scaling law.

Keywords : Density Fluctuation, Anomarous Transport, Interferometer, Scattering, Diffusion Coefficient, DTEM, JFT-2

+ Division of Large Tokamak Development, Tokai Research Establishment, JAERI

マイクロ波干渉法および散乱法による JFT−2プラズマの密度揺動の測定

日本原子力研究所東海研究所核融合研究部

荘司　昭朗・山本　巧・船橋　昭昌

嶋田　道也[+]・藤沢　登[+]・河上　知秀

（1981年10月21日受理）

トカマクの異常輸送と関係する密度揺動をマイクロ波干渉法および散乱法によって測定した。干渉法による最大の揺動振巾は10^{-2}のオーダであり，又，散乱法による波数K⊥=28.6 cm^{-1}における揺動の大きさは10^{-3}のオーダであった。散逸性補獲電子（DTEM）不安定性の理論に測定値を代入して求めた拡散係数は，実験的に求めた値と一致する。DTEM不安定性の増大率と密度揺動の振巾から求められる，密度に反比例する拡散係数の依存性は，経験的なスケーリングと一致する。

＋　大型トカマク開発部

Contents

目　　次

1. Introduction

In recent experiments of electromagnetic waves scattering from collective modes in the ATC[1] and TFR[2] tokamaks, smallscale density fluctuations were investigated in relation with anomalous transport in a plasma. However, no measurement of the entire wave vector spectrum on all positions was carried out in their experiments. In the present paper, we report an experimental observation of the density fluctuations measured by two methods; interferometer and scattering system of 4 mm microwave at various positions. The diffusion coefficient estimated by using DTEM theory from the density fluctuation is compared with the experimental value. We describe the measurement by microwave interferometer in Section 2 and the measurement by microwave scattering method. In Section 3, we discuss the anomarous transport due to electron density fluctuation.

2. Measurement by micrówave interferometer

The block diagram of interferometer measurement is shown in Fig. 1. Transmiting and receiving horn can be horizontally scaned with width of interval 6 cm from 24 cm (out side) to -18 cm (inside). A homodyne detection system is used in which the received wave is mixed with a reference wave directly from Klystron (70 GHz). The signal from a crystal detecor is sampled by transient recorder (2000 times with a sampling frequency of 5MHz), stored in a disk memory and magnetic tape, and analyzed by programs of auto-corretion and Fourier transformation. The ports of lower sampling frequency (500 kHz) are for monitor of zeroth order phase shift ϕ_0 by mean of electron density and MHD instabilities.

The high frequency components of the detected signal $S_1(t)$ are related to phase change $\tilde{\phi}_i$ due to density fluctuations[3)]

$$\left.\begin{aligned} S_i(t) &= A\,\tilde{\phi}_1\, E_i E_1 \sin(\alpha_0+\alpha_1) \\ \tilde{\phi}_1 &= \frac{\beta_0}{2}\frac{1}{X_H}\int dx \int \tilde{n}\ (x, z, t)\, dz, \end{aligned}\right\} \qquad (1)$$

where E_i, E_1 are strength of incident and reference microwave, α_0, α_1 are phase shifts by plasma and circuit, β_0 is the free space wave number of the incident wave, x_H is the horn width, x indicates the horizontal position, and $\tilde{n}$ (x,z,t) is the instantaneous electron density fluctuations. The integration over x in Eq. 1 shows that we must take mean on the width of horn for the case of instabilities with wave length λ smaller than horn width. We may consider that $\tilde{\phi}_1$ is represented by following quantity

$$\tilde{\phi}_1 = \frac{\beta_0}{2}\int \tilde{n}\,\frac{\lambda_x}{X_H}\,dx \qquad (2)$$

wher λ_x is the x component of wave length of instability. In practice, rotating a tephlon sheet (specific permittivity $\varepsilon_s = 2$) of 2 mm thickness with comb-tooth $\lambda = 2 \sim 130$ mm between two horns, we have experimentally this dependence on wave length that saturates at $\lambda \simeq x_H$, as shown in Fig.2.

The detected signals are taken into auto-corretion $\varphi(\tau)$ and Fourier transformation;

$$\left.\begin{aligned} \varphi(\tau) &= \int S_1(t)\ S_1(t+\tau)\ dt\ , \\ &= \int S_\omega^2\ e^{-i\omega\tau}\ d\omega \\ S_\omega^2 &= \frac{1}{2\pi}\int \varphi(\tau)\ e^{i\omega\tau}\ d\tau \end{aligned}\right\} \qquad (3)$$

In specific, $\varphi(0)$ is the total power density ($\varphi(0) = \int S_\omega^2\, d\omega$). Practically, we calculated auto-correlation for each block of 500 data (2000 data devided to four blok) and averrage statistically about several shots ($<S_\omega^2>$).

The power spectra obtained in typical three discharges are shown in Fig. 3, in which R=90 cm, $n_e(0)=2\times10^{13}$ cm^{-3}

(A) B_t=9 kG, a=25 cm, $T_e(0)$=680 eV, $T_i(0)$=200 eV, $\nu_{*\,min}$=2

(B) B_t=18 kG, a=25 cm, $T_e(0)$=1.2 keV, $T_i(0)$=270 eV, $\nu_{*\,min}$=0.8

(C) B_t=18 kG, a=17 cm, $T_e(0)$=800 eV, $T_i(0)$=270 eV, $\nu_{*\,min}$=2

where $\nu^*$is the ratio of collision frequency to baunce frequency. The range of observed frequencies (50 kHz～500 kHz) is that of drift wave with maximum growth rate at $k_\perp \rho_i \sim 0.5$. A frequency dependence of spectra is nealy $<S_\omega^2> \sim f^{-2.5}$.

The spacial distribution of total power density for these three cases are shown in Fig.4. A considable asymmetry between the outside and the inside of the torus is observed. One possible explanation of this asymmetry is given by the ballooning effect of the disspative trapped electron mode[4]. We consider a model such as the drift wave distribute at $r=r_0$ with the eigen function $g(\theta)=1+A\cos\theta$ and localization width Δ,

$$\tilde{n} = |\tilde{n}|\,\delta(r-r_0)\cdot g(\theta)\cdot \sin(\omega t - m\theta)\,. \qquad (4)$$

Substituting Eq. (4) into Eq. (1) and using aproximations of $\Delta/r_0 \ll 1$, $X_H/r_0 \ll 1$, and $m>1$, we have

$$\left.\begin{aligned} \tilde{\phi}_1 &= \frac{\beta_0}{2}\,\frac{r_0\Delta}{X_H}\cdot\frac{|\tilde{n}|}{m}\,F(\theta_0)\,\sin\omega t\ , \\ S_\omega^2 &\propto |\tilde{n}|^2\,(1+AX/r_0)^2/k_\perp^2 \end{aligned}\right\} \qquad (5)$$

The calculational results of frequency spectra from Eq. (5) are also drawn in Fig.4.

Considering $S_\omega \propto \int \tilde{n}/k_\perp \, dz$ in Eqs. (1), (2) with $k_\perp \sim k_x$, we make the asymmetry abel inversion and obtain the distribution of $\Sigma (\tilde{n}/k_\perp)^2$ (Fig.5)[5]. The maximum amplitude of the density fluctuations at x=18cm for the case B is about 10^{-2} of the mean electron density, which measured by comparing it with output per half fringe.

We also get experimentally the density dependence of the fluctuation powers for the case of following experimental conditions; B_T=14kG, a=25cm, $T_e(0)$=800eV
(a) $n_e(0)=2\times10^{13}cm^{-3}$, $T_i(0)$=240eV, (b) $n_e(0)=2.8\times10^{13}cm^{-3}$, Ti(0)= 280eV, (c) $n_e(0)=4\times10^{13}cm^{-13}$, $T_i(0)$=320eV (Fig.6). From this results, the maximum fluctuation powers are nearly independent on the mean electron density;

$$\left.\begin{aligned} &\Sigma\langle S_\omega^2\rangle \sim \left(\frac{\tilde{n}\,\max}{k_\perp}\right)^2 \sim \text{const.} \\ &\frac{\tilde{n}}{\bar{n}} \sim \frac{k_\perp}{\bar{n}} \end{aligned}\right\} \qquad (6)$$

The width of localization have a tendency to decrease with increasing the density.

3. Measurment by microwave scattering method

The array of antennae shown in Fig.7 has been used for launching a microwave of frequency $\omega_i/2\pi \simeq 70$ GHz into a plasma and for collecting waves which are scattered by density fluctuations. The wave, which has its electric field parallel to the toroidal magnetic field, is transmitted through a horn antenna movable along the major radius direction in order to scan the illuminating position. The scattered microwaves are picked up by another horn antenna placed inside the vaccum vessel. Its horn is aimed at an angle of 135° with the direction of the incident wave. The component of the density fluctuation having the wave number $|\vec{k}| = |\vec{k}_i - \vec{k}_s|$ ($\vec{k}_i$ and $\vec{k}_s$ being the wave vector of the incident and the scattered waves, respectively, and both being perpendicular to the toroidal magnetic field) is selectively detected.

A homodyne detection system is used in which the received wave is mixed with a larger reference wave directly from the microwave oscillator. The signal from a crystal mixer is amplified and fed to the data processing system mentioned above, in which the frequency power spectrum is calculated.

The frequency spectra of the signals measured at different regions are shown in Fig.8. The observed spectra are produced by fluctuations which have both components of azimuthal and radial wave numbers. These results are obtained in a typical discharge condition; B_t=18 kG, I_p=160 kA, a=25 cm, q_a=4, $\bar{n}_e \simeq 1.3\times10^{13}$cm^{-3}, $T_e(0) \simeq 1.2$ keV, $T_i(0) \simeq 350$ eV, Z_{eff}=4~5.

The range of the observed frequencies is that of the drift waves. However, the obtained frequency spectra do not show the peak at the frequency expected from the linear dispersion relation of the drift wave, $\omega \simeq \omega^*$ (see Fig.9). Figure 8 indicates that the power law dependence of the turbulent fluctuations is of the form $(\tilde{n}_e/n_e)^2 \propto f^{-1.8\sim-2.5}$ for any position.

The amplitude of density fluctuations, $<|\tilde{n}_e(k_\perp)/n_e|^2>^{1/2} = <\int|n_e(k_\perp,\omega)/n_e|^2 d\omega/2\pi>^{1/2}$ is shown Fig.10. for the different scattering positions. The measured level of drift wave turbulence is of the order of 10^{-3} and is somewhat less than that predicted by a strong turbulent theory. According to Kadomtsev[6], when strong turbulence develops the oscillation amplitude increases to $(L_n k_r)^{-1}$

where $L_n = d(\ln n_e)/dr$. The calculated values of $(L_n k_r)^{-1}$ at the different positions are shown in Fig.10.

4. Discussions

We estimate the order of the diffusion coefficient of the case B discharge in the paragraph 2. The particle diffusion by the electrostatic density fluctuations can be derived from the following relations,[7]

$$\left.\begin{aligned} \tilde{D}_e &\simeq \Sigma \frac{\gamma}{L_n^2}\left(\frac{\tilde{n}}{n}\right)^2 \\ \gamma &\simeq \varepsilon^{1/2}\ \omega_e^{*2}\ \eta\ \nu_{eff} \,/\, (\omega_e^{*2} + \nu_{eff}^2) \end{aligned}\right\} \qquad (7)$$

where $\eta = d \ln T_e / d \ln n$, $\nu_{eff} \simeq \nu_{ei}/\varepsilon$ and ω_e^* is the drift frequency. For our case, $\tilde{n}_{max}/\bar{n} \sim L_n/k_\perp \sim 10^{-2}$, $\omega^{Exp} \sim \omega_e^* \sim 10^6/s$ ($k_\perp \rho_i \simeq 0.5$), $L_n \sim 10^{-1} cm^{-1}$, $\eta \sim 2$, $\gamma \sim 10^5/s$, $k_\perp \sim 5 cm^{-1}$ and $\tilde{D}_e \sim 10^4 cm^2/s$ (Fig.11, 12). Value of diffusion coefficient is the same order with that which is got by the spectroscopic measurements.

In order that the density dependence of the fluctuation amplitudes ($\tilde{n}/\bar{n} \sim k_\perp/\bar{n}$) are compatible with the relation of satulation level ($\tilde{n}/n \sim L_n/k_\perp$), the wave number must be propcrtional to the square root of mean electron density, that is, $k_\perp \sim \sqrt{L_n \bar{n}}\ \sqrt{\bar{n}}$. Therefore,

$$\tilde{D}_e \sim \varepsilon^{1/2} \eta \omega^{*2} / \nu_{ei} \left(\frac{\tilde{n}}{n}\right)^2 \Big/ L_n^2 \sim \frac{1}{\bar{n}} \qquad (8)$$

and this dependence is consistent with the empirical scaling.

Acknowledgement

We are grateful to members of JFT-2, diagonostic and operating groups for their discussions and efforts. We also would like to express our gratitude to Drs. Y. Tanaka, M. Tanaka and Y. Obata for their contionuous encouragement to the present work.

4. Discussions

We estimate the order of the diffusion coefficient of the case B discharge in the paragraph 2. The particle diffusion by the electrostatic density fluctuations can be derived from the following relations,[7]

$$\left.\begin{aligned} \tilde{D}_e &\simeq \Sigma \frac{\gamma}{L_n^2}\left(\frac{\tilde{n}}{n}\right)^2 \\ \gamma &\simeq \varepsilon^{1/2}\ \omega_e^{*2}\ \eta\ \nu_{eff} \,/\, (\omega_e^{*2} + \nu_{eff}^2) \end{aligned}\right\} \qquad (7)$$

where $\eta = d \ln T_e / d \ln n$, $\nu_{eff} \simeq \nu_{ei}/\varepsilon$ and ω_e^* is the drift frequency. For our case, $\tilde{n}_{max}/\bar{n} \sim L_n/k_\perp \sim 10^{-2}$, $\omega^{Exp} \sim \omega_e^* \sim 10^6/s$ ($k_\perp \rho_i \simeq 0.5$), $L_n \sim 10^{-1} cm^{-1}$, $\eta \sim 2$, $\gamma \sim 10^5/s$, $k_\perp \sim 5 cm^{-1}$ and $\tilde{D}_e \sim 10^4 cm^2/s$ (Fig.11, 12). Value of diffusion coefficient is the same order with that which is got by the spectroscopic measurements.

In order that the density dependence of the fluctuation amplitudes ($\tilde{n}/\bar{n} \sim k_\perp/\bar{n}$) are compatible with the relation of satulation level ($\tilde{n}/n \sim L_n/k_\perp$), the wave number must be proportional to the square root of mean electron density, that is, $k_\perp \sim \sqrt{L_n \bar{n}}\ \sqrt{\bar{n}}$. Therefore,

$$\tilde{D}_e \sim \varepsilon^{1/2} \eta \omega^{*2} / \nu_{ei} \left(\frac{\tilde{n}}{n}\right)^2 \Big/ L_n^2 \sim \frac{1}{\bar{n}} \qquad (8)$$

and this dependence is consistent with the empirical scaling.

Acknowledgement

We are grateful to members of JFT-2, diagonostic and operating groups for their discussions and efforts. We also would like to express our gratitude to Drs. Y. Tanaka, M. Tanaka and Y. Obata for their contionuous encouragement to the present work.

References

(1) Goldston, R.J., Mazzucato, E., Slusher, R.E., Surko, C.M., in Plasma Physics and Controlled Nuclear Fusion Research (Proc. 6th Int. Conf. Berchtesgaden, 1976) 1, IAEA, Vienna (1977) 371.

(2) TFR Group, ibid. 1 35.

(3) Pawer E.J. et. al ; Journal of Appl. Phys. 47, 9 (1976) 3911.

(4) Liewer P.C. et. al ; Phys. Fluids 19, (1976) 276.

(5) Matoba T. et. al ; JAERI-M 6239 (1975)

(6) Kadomtsev B.B ; Plasma Turbulence, (Academic Press New York 1965), chap. 4

(7) Kadomtsev et. al.; Nucl. Fusion 11, (1971) 67.

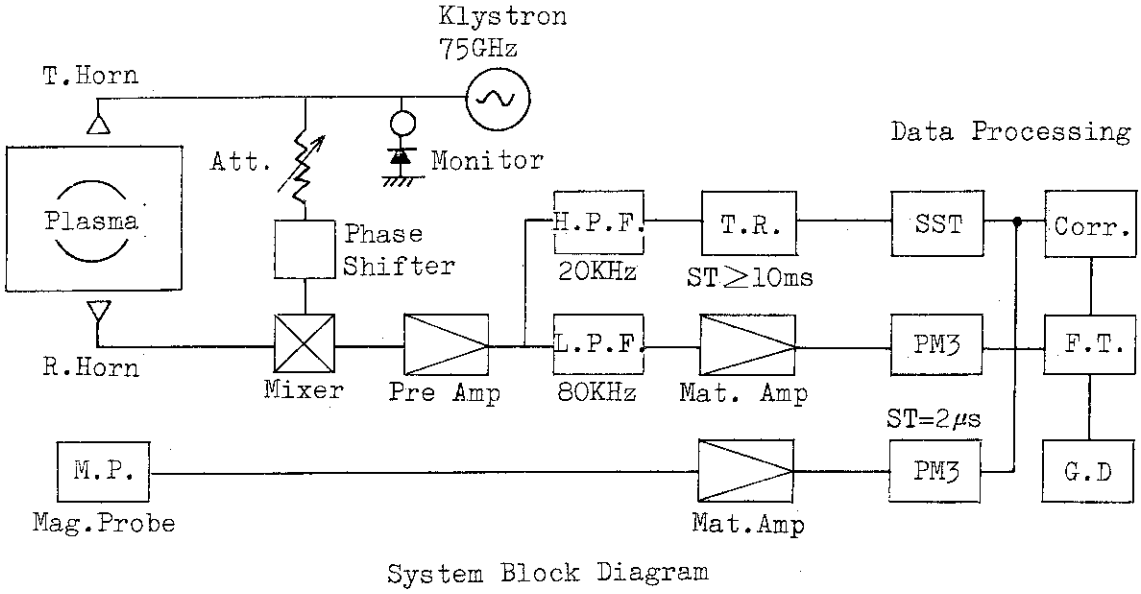

Fig.1 The block diagram of the interferometer measurement system.

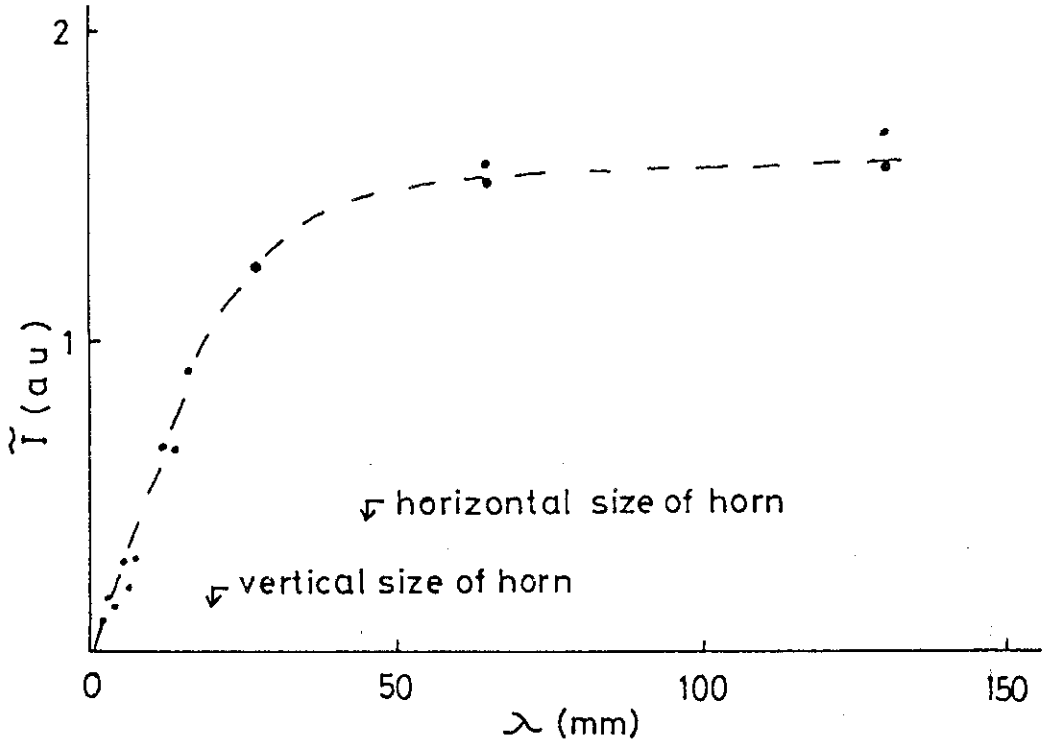

Fig.2 The dependence of interferometer output on the wave length by model experiment of a tephlon sheet with comb-tooth.

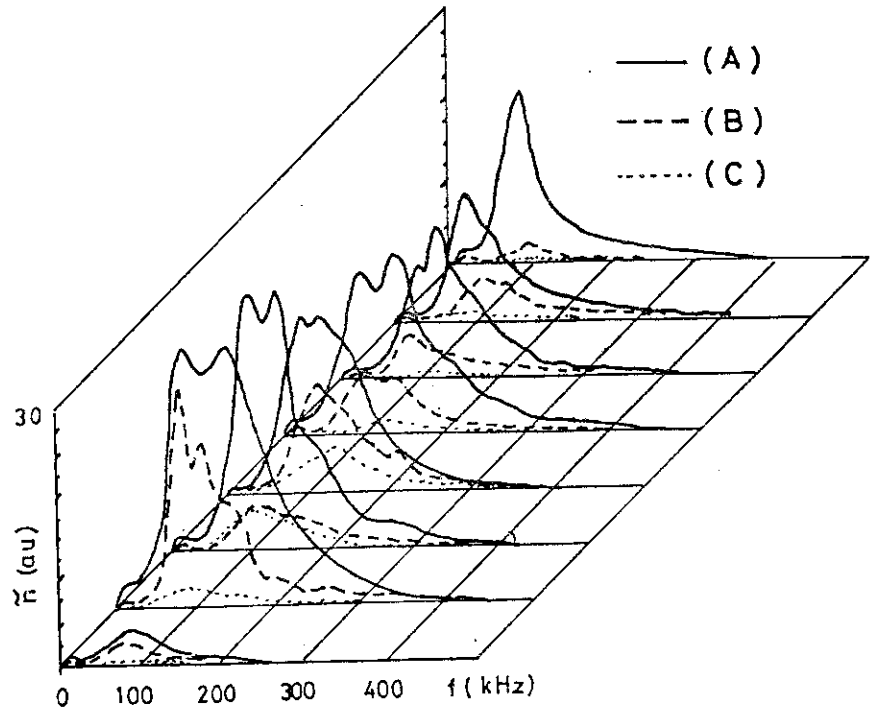

Fig.3 The frequency spectra in typical three discharges; $n_e(0)=2\times10^{13}$ cm^{-3}, (A) B_T=9kG, (B) B_T=18kG, a=25cm, (C) B_T=18kG, a=17cm.

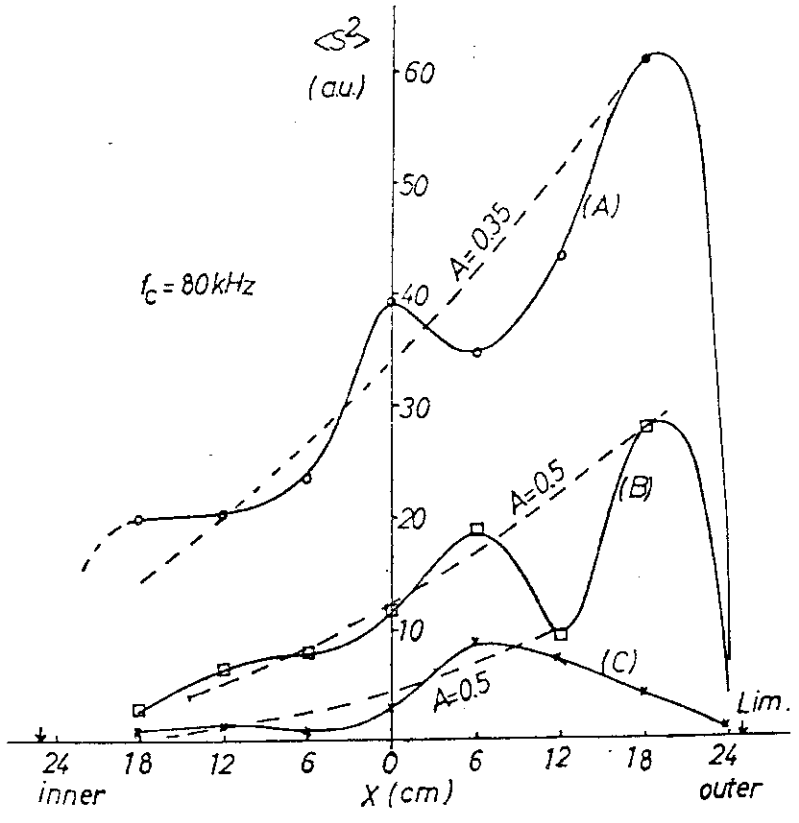

Fig.4 The spacial distributions of the total power density. Dotted curves show the calculational result with the balooning effect.

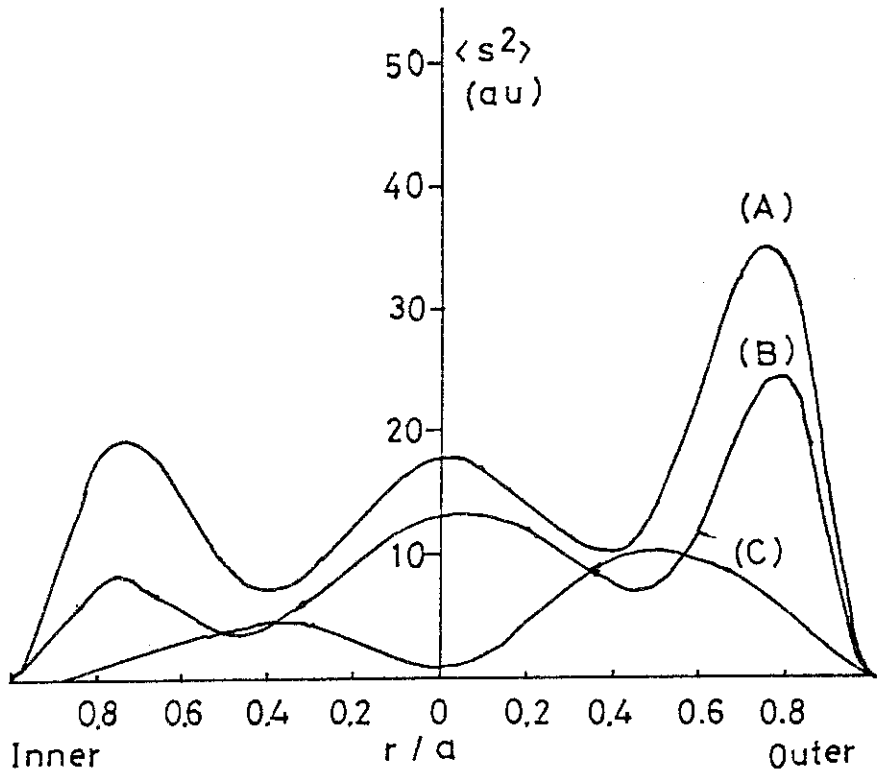

Fig.5 The spacial distributions of the quantity obtained by the asymmetry abel invertion.

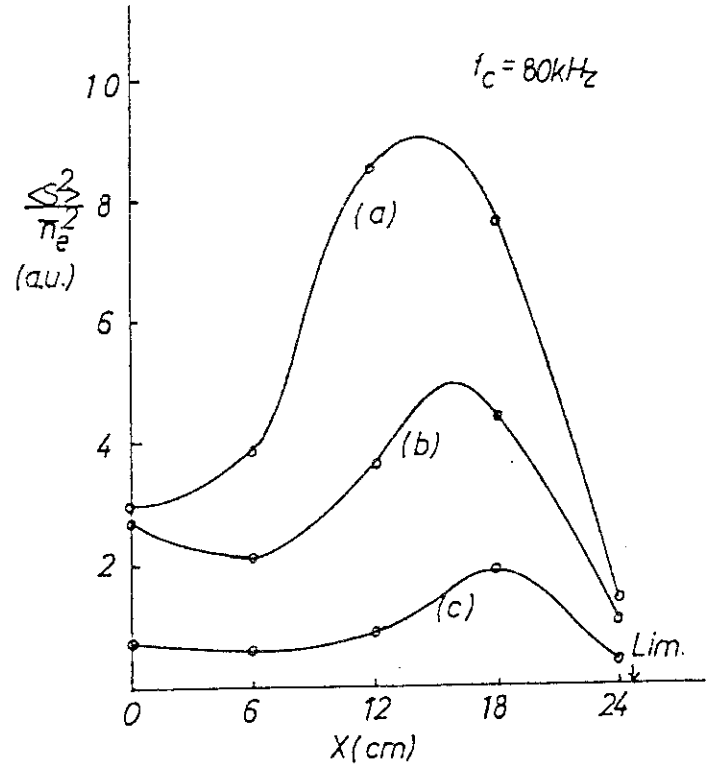

Fig.6 The density dependence of power distributions of fluctuations in dichage conditions; B_T=14kG, a=25cm. (a) $n_e(0)=2\times10^{13}cm^{-3}$, (b) $n_e(0)=2.8\times10^{13}cm^{-3}$, (c) $n_e(0)=4\times10^{13}cm^{-3}$.

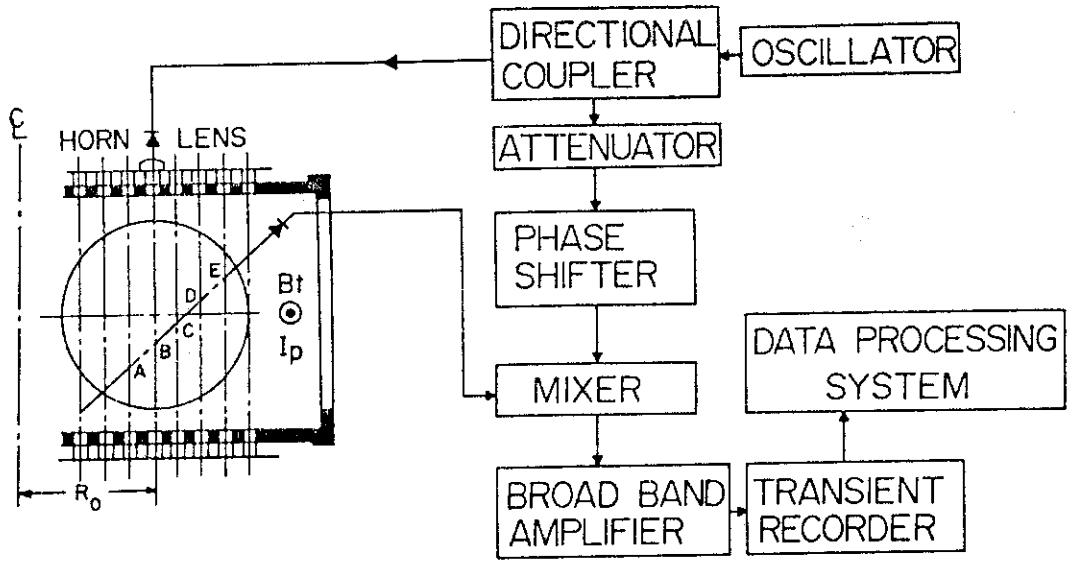

Fig.7 Experimental apparatus for microwave scattering. An antenna on the top was used for launching the wave and is movable along the major radius direction. An another antenna on the side was used for collecting the scattered waves. The hatched area is the effective scattering region.

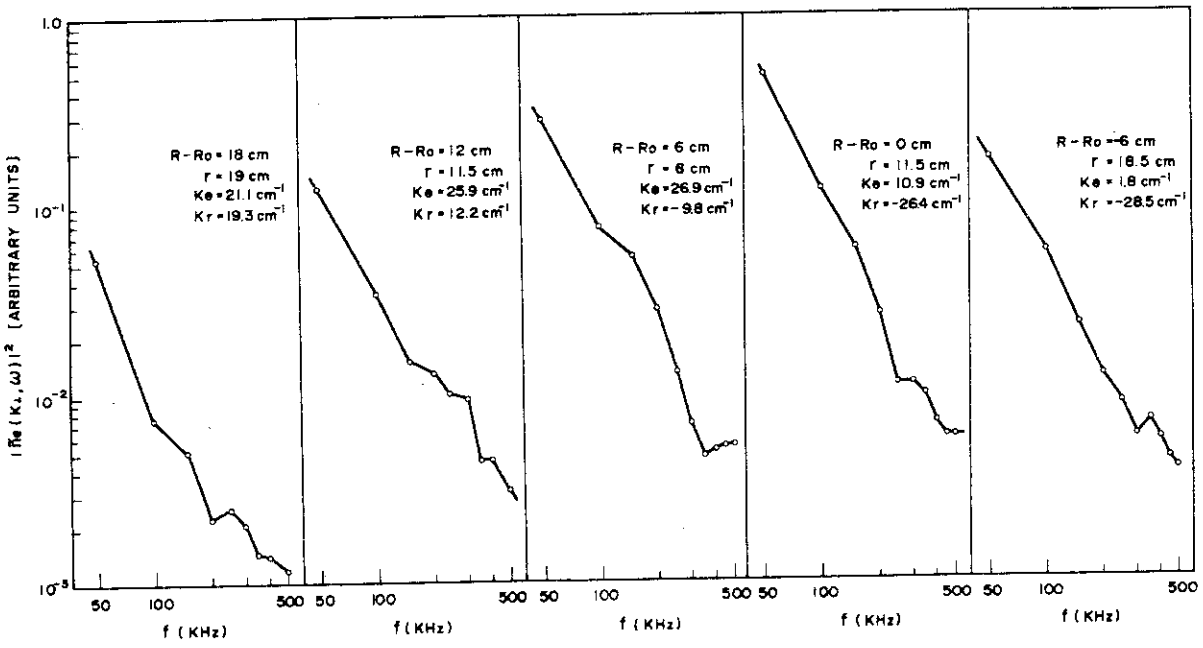

Fig.8 The frequency power spectra of microwave signals produced by electron density fluctuations at different regions of the plasma column.

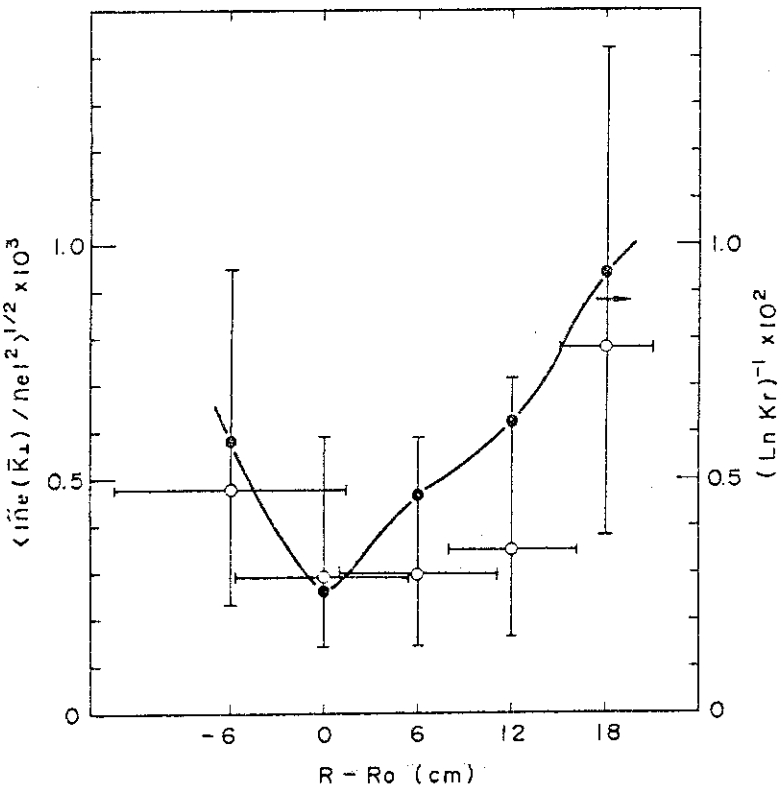

Fig.10 The amplitude of density fluctuations at the different scattering regions. The open circule indicates the measured value and the solid circule indicates the value of $(L_n k_r)^{-1}$ where $L_n = d\ln n_e/dr$.

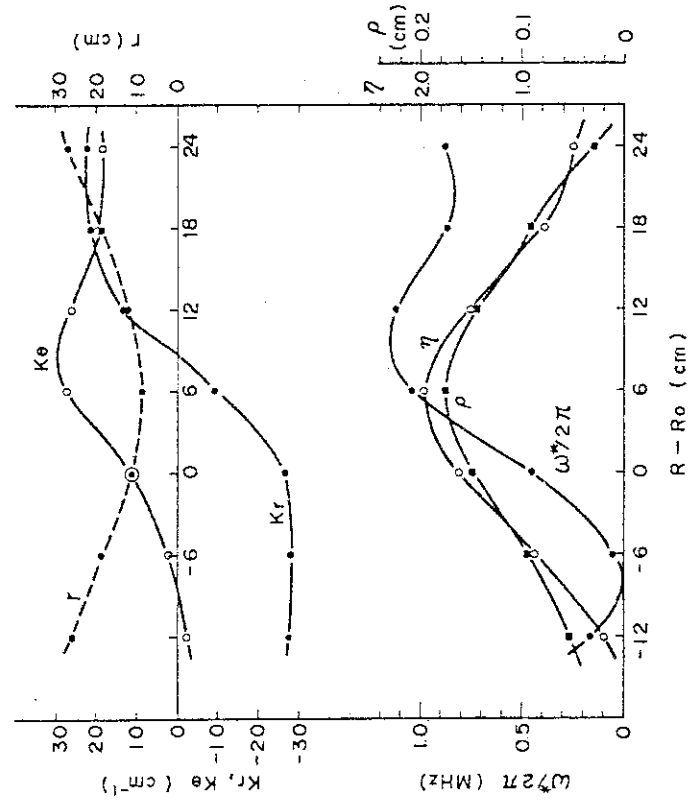

Fig.9 Characteristic parameters of instrument and plasma versus the major radius. The k_θ and k_r are the azimuthal and radial wave numbers and r is the minor radius, $\omega^* \equiv (k_\theta T_e/eB)(d\ln n_e/dr)$ is the electron diamagnetic drift frequency and $\eta_e \equiv d\ln T_e/d\ln n_e$.

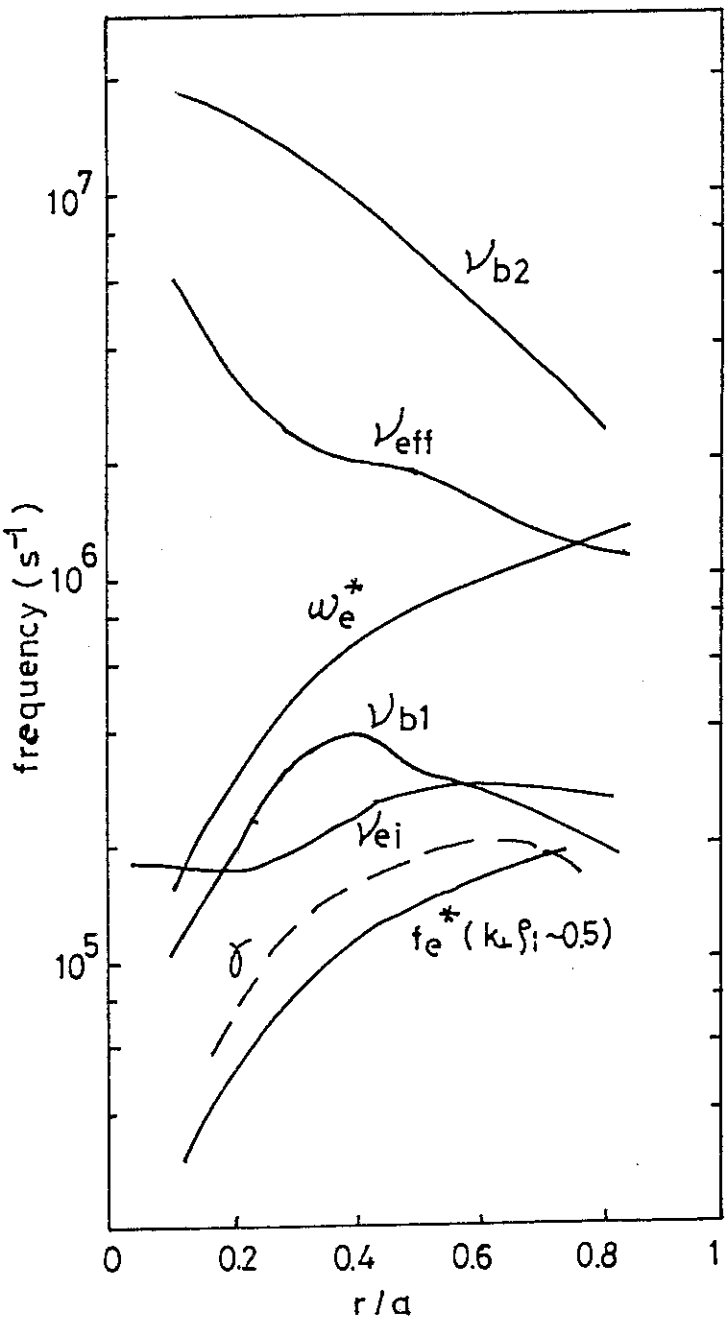

Fig.11 The frequency parameters in the case B.

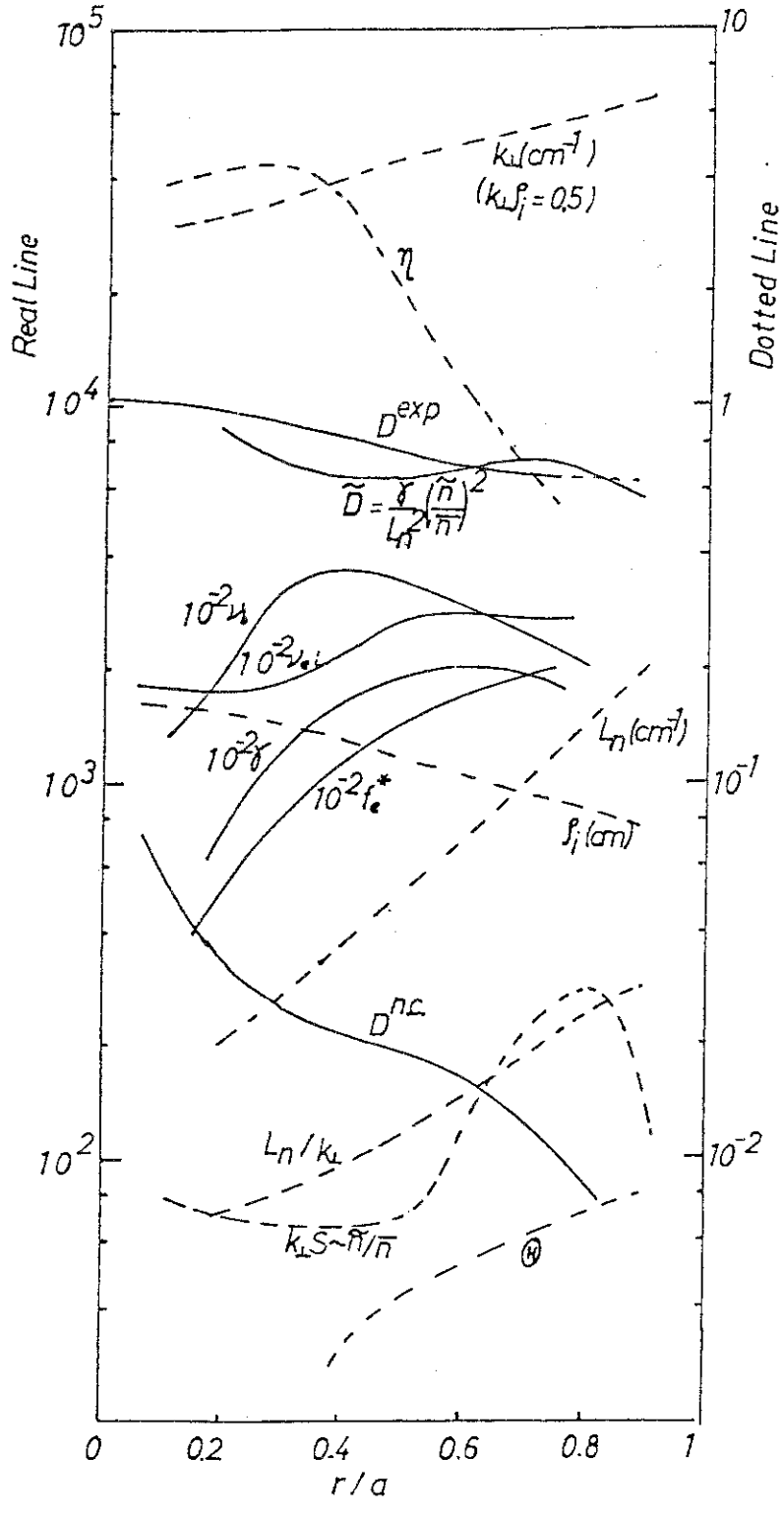

Fig.12 The various parameters relating with the transport coefficient in the case B.